

## Accepted Manuscript

Discovery of 2-((1*H*-benzo[*d*]imidazol-1-yl)methyl)-4*H*-pyrido[1,2-*a*]pyrimidin-4-ones as Novel PKM2 Activators

Chuangxing Guo, Angelica Linton, Mehran Jalaie, Susan Kephart, Martha Ornelas, Mason Pairish, Samantha Greasley, Paul Richardson, Karen Maegley, Michael Hickey, John Li, Xin Wu, Christy Ji, Zhi Xie

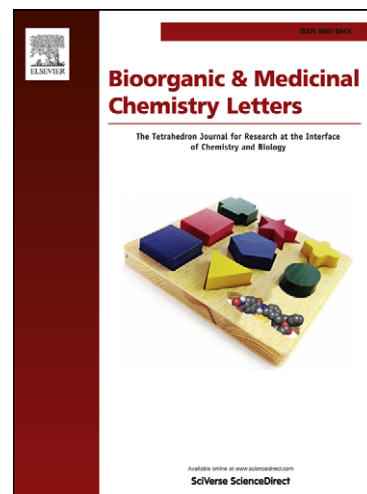
PII: S0960-894X(13)00418-6  
DOI: <http://dx.doi.org/10.1016/j.bmcl.2013.03.090>  
Reference: BMCL 20326

To appear in: *Bioorganic & Medicinal Chemistry Letters*

Received Date: 4 February 2013  
Revised Date: 20 March 2013  
Accepted Date: 22 March 2013

Please cite this article as: Guo, C., Linton, A., Jalaie, M., Kephart, S., Ornelas, M., Pairish, M., Greasley, S., Richardson, P., Maegley, K., Hickey, M., Li, J., Wu, X., Ji, C., Xie, Z., Discovery of 2-((1*H*-benzo[*d*]imidazol-1-yl)methyl)-4*H*-pyrido[1,2-*a*]pyrimidin-4-ones as Novel PKM2 Activators, *Bioorganic & Medicinal Chemistry Letters* (2013), doi: <http://dx.doi.org/10.1016/j.bmcl.2013.03.090>

This is a PDF file of an unedited manuscript that has been accepted for publication. As a service to our customers we are providing this early version of the manuscript. The manuscript will undergo copyediting, typesetting, and review of the resulting proof before it is published in its final form. Please note that during the production process errors may be discovered which could affect the content, and all legal disclaimers that apply to the journal pertain.

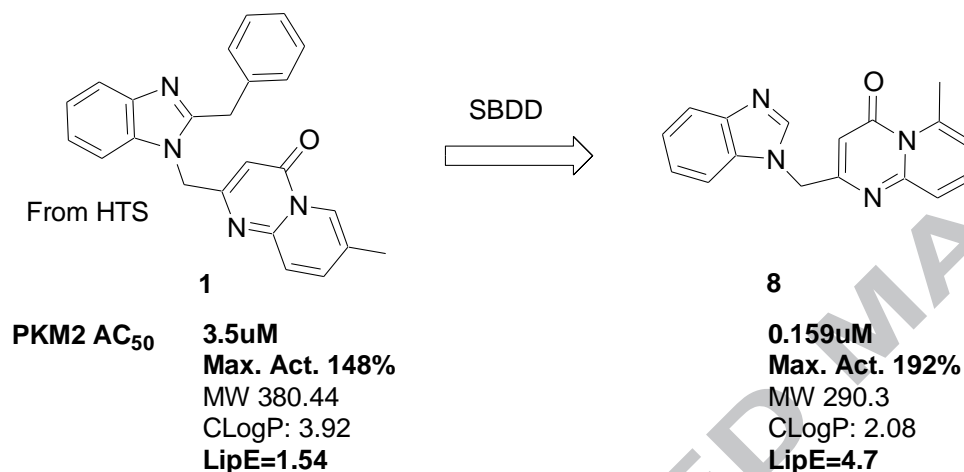


## Graphic Abstract

## Discovery of 2-((1*H*-benzo[*d*]imidazol-1-yl)methyl)-4*H*-pyrido[1,2-*a*]pyrimidin-4-ones as Novel PKM2 Activators

Chuangxing Guo,\* Angelica Linton,\* Mehran Jalaie, Susan Kephart, Martha Ornelas, Mason Pairish, Samantha Greasley, Paul Richardson, Karen Maegley, Michael Hickey, John Li, Xin Wu, Christy Ji, Zhi Xie

*Pfizer Global Research and Development, 10770 Science Center Drive, San Diego, CA 92121*



2-((1*H*-benzo[*d*]imidazol-1-yl)methyl)-4*H*-pyrido[1,2-*a*]pyrimidin-4-ones were identified as novel PKM2 activators with a novel binding mode. The original lead was optimized into an efficient series via computer-aided structure-based drug design. Biological studies on the representative PKM2 activators suggest that PKM2 activation alone is not sufficient to alter cancer cell metabolism.

## Discovery of 2-((1*H*-benzo[*d*]imidazol-1-yl)methyl)-4*H*-pyrido[1,2-*a*]pyrimidin-4-ones as Novel PKM2 Activators

Chuangxing Guo,\* Angelica Linton,\* Mehran Jalaie, Susan Kephart, Martha Ornelas, Mason Pairish, Samantha Greasley, Paul Richardson, Karen Maegley, Michael Hickey, John Li, Xin Wu, Christy Ji, Zhi Xie

*Oncology Medicinal Chemistry, Pfizer Worldwide Research & Development, San Diego, CA 92121, USA*

**Abstract** The M2 isoform of pyruvate kinase is an emerging target for antitumor therapy. In this paper, we describe the discovery of 2-((1*H*-benzo[*d*]imidazol-1-yl)methyl)-4*H*-pyrido[1,2-*a*]pyrimidin-4-ones as potent and selective PKM2 activators which were found to have a novel binding mode. The original lead identified from high throughput screening was optimized into an efficient series via computer-aided structure-based drug design. Both a representative compound from this series and an activator described in the literature were used as molecular tools to probe the biological effects of PKM2 activation on cancer cells. Our results suggested that PKM2 activation alone is not sufficient to alter cancer cell metabolism.

In recent years there has been increased interest in the mechanisms of fundamental metabolic alterations during malignant transformation. The reprogramming of cellular energy to support abnormal growth and proliferation of cancer cells is considered an emergent hallmark of cancer.<sup>1</sup>

Understanding the biological differences between normal cells and cancer cells is crucial for formulating strategies to treat cancer. More than 75 years ago the observation was made that tumor cells have an elevated rate of glucose uptake but reduced rates of oxidative phosphorylation,<sup>2</sup> now known as the Warburg effect. Recently, the involvement of the M2 splice isoform of pyruvate kinase in the shift in cellular metabolism to aerobic glycolysis has been proposed.<sup>3</sup> Tumor cells exclusively express the embryonic M2 isoform of pyruvate kinase (PKM2),<sup>4</sup> which can switch from a less active dimeric form to a highly active tetrameric form. PKM2 is proposed to shuttle between these two forms to regulate the metabolism of glucose. The low activity dimeric form supports cell growth by increasing glycolytic intermediates necessary for biosynthetic processes, but when energy levels fall, the enzyme can switch to the high activity tetrameric form and facilitate oxidative phosphorylation.<sup>3,4</sup> While it has been reported that PKM2 in tumors exists predominantly as the less active dimer, the exact mechanism of its involvement in tumorigenesis and the Warburg effect is still not well understood. Consequently, there

have been significant research efforts to elucidate pyruvate kinase regulation and to assess PKM2 as a target for cancer therapy.<sup>5</sup>

Christofk et al.<sup>3</sup> showed that switching pyruvate kinase expression to the M1 isoform results in a reversal of the Warburg effect, as measured by reduced lactate production and increased oxygen consumption. These observations correlated to a reduced ability to form tumors in nude mouse xenografts.<sup>5d</sup> It has been hypothesized that pharmacological intervention to restore the activity of tumor PKM2 to levels seen with PKM1 in normal cells may force cancer cells to adopt a metabolic state characteristic of normal cells, thus suggesting PKM2 activation as a novel strategy to inhibit tumor growth. Several small molecule activators of PKM2 have been reported in literature.<sup>6</sup>

Here we report the discovery of a series of pyridopyrimidinone analogs as potent activators of PKM2 with good HLM stability,<sup>7</sup> permeability, solubility and selectivity. Lead compounds resulting from our discovery program were used as tool molecules to probe the effects of PKM2 activation on cancer cell metabolism and proliferation. The resulting structure-activity relationships, effects on oxygen consumption and lactate production, and cancer cell proliferation are discussed.

PKM2 catalyzes the conversion of phosphoenolpyruvate (PEP) to pyruvate and generates ATP in the process. A high-throughput screening (HTS) assay that monitored production of ATP by luminescence was developed, and Compound **1** (Figure 1) was identified as one of the most active hits, showing 155% activation at 10  $\mu$ M. The active compounds in the HTS assay were further characterized using a lactate dehydrogenase (LDH)-coupled enzyme assay. In this assay, Compound **1** gave an AC<sub>50</sub> of 3.5  $\mu$ M and a maximal activation of 148% compared to FBP.<sup>8</sup> Compound **1** was subsequently modeled<sup>9</sup> into the activator binding site of the published PKM2 co-crystal structure (Figure 1).<sup>10</sup> According to previous reports, the activator binding site is located at the dimer-dimer interface.<sup>5e</sup> In this model of Compound **1**, it appeared that the benzyl group presented a sub-optimal interaction with the PKM2 protein and in order to accommodate the benzyl group, two water molecules which are part of a H-bond network to the carbonyl main chain of ASN350 need to be displaced. However, these water molecules are part of an intricate network of H-bonds, and displacement by the benzyl moiety would leave an unsatisfied H-bond network (generating a desolvation penalty), ultimately leading to suboptimal binding affinity of Compound **1**.

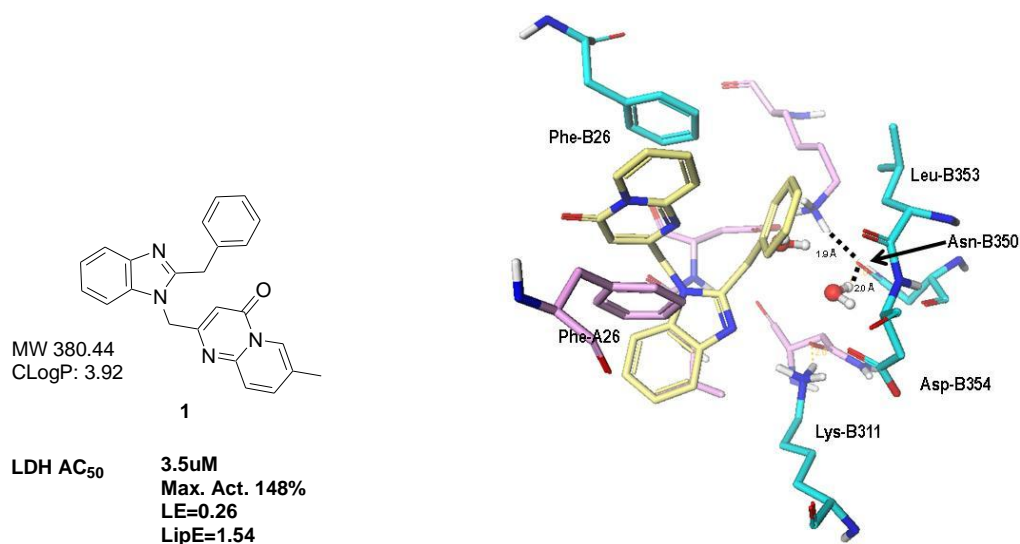


**Figure 1** Compound **1** modeled into the reported activator binding site. Compound **1** (yellow) is docked into the activator binding site of published PKM2 co-crystal structure PDB IDs = 3GQY.

Several simple analogs were designed and synthesized to test the effect of replacing the sub-optimal benzyl group with a smaller substituent. The analog lacking the phenyl group lost biochemical activity (**2**, Figure 2, max. activation: 73% @ 10  $\mu$ M), but further removal of the C-2 methyl substituent resulted in a 5.4 fold improvement in potency (**3**, Figure 2,  $AC_{50}$  = 755 nM). The simple unsubstituted core was found to be 10-fold more potent in the PKM2 activation assay (**4**,  $AC_{50}$  = 340 nM, Figure 2), leading to a significant increase in efficiency (LipE = 5.14 vs 1.54)<sup>11</sup> compared to the original HTS hit **1**.

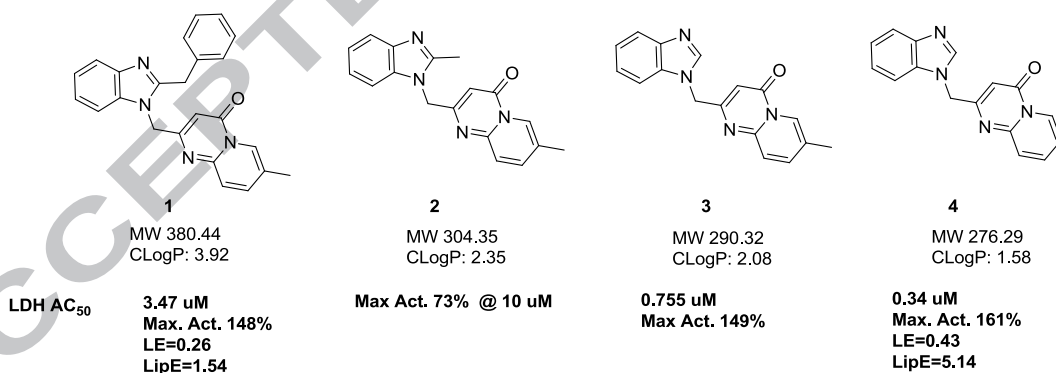


**Figure 2.** Initial optimization of HTS Pyridopyrimidinone lead **1**.

An X-ray co-crystal structure of Compound **4**<sup>12</sup> with PKM2 protein was solved, revealing the binding conformation (Figure 3). When compared to several published co-crystal structures including 3GR4 / 3H6O / 3GQY, (Figure 3),<sup>13</sup> the 2-((1*H*-benzo[*d*]imidazol-1-yl)methyl)-4*H*-pyrido[1,2-*a*]pyrimidin-4-one core of compound **4** adopts a unique binding mode. The benzimidazole fragment

reaches a region of the activator pocket that is not occupied by an activator in any of the published crystal structures. Furthermore, one of the imidazole nitrogens forms a hydrogen-bond to LYS311 which is normally part of a salt bridge to ASP354. Such an interaction has not been observed in other published co-crystal structures. In general, the ligand is bound to the activator site in two separate conformations with equal occupancy, with the core rotated by 47 degrees in relation to other activators.<sup>14</sup> For simplicity figure 3 shows only the ligand bound to the A/B dimer activator site and not the one bound to the C/D dimer. The pyrimidone ring sits between the two Phe26 residues from monomers A (pink) and B (cyan) forming  $\pi$ - $\pi$  interactions among the aromatic rings. The carbonyl interacts with a bridging water molecule, which in turn interacts with the carbonyl of the backbone of TYR390 (Figure 4). The observation of a new binding mode presented new opportunities for the design of more potent PKM2 activators.

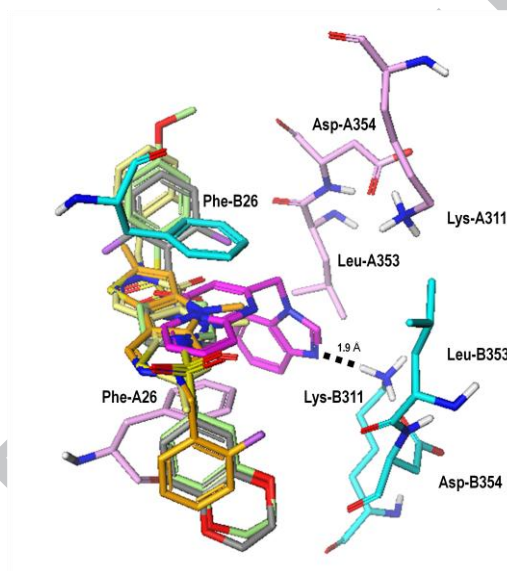
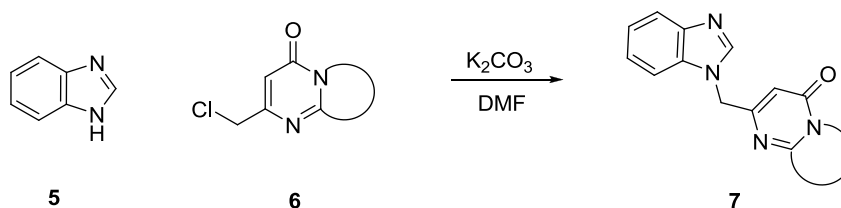


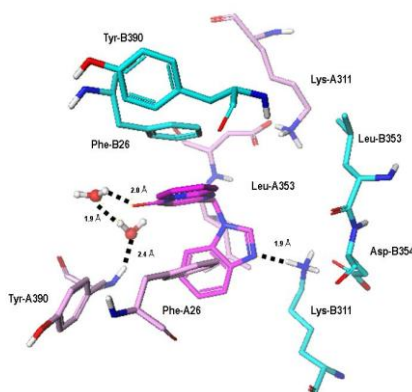
**Figure 3.** Comparison of X-Ray co-crystal structure of compound **4** (PDB: 4JPG, magenta) and published activator structures 3GR4 (gray) / 3H6O (orange) / 3GQY (green). PKM2 monomer A (pink), PKM2 monomer B (cyan).

The preparation of these pyridopyrimidinone analogs is outlined in **Scheme 1**. Nucleophilic displacement of various commercially available 6-(chloromethyl)pyrimidines **6** with the anion of 1*H*-benzimidazole **5**<sup>15</sup> provides compounds of the general structure **7** in good yields.



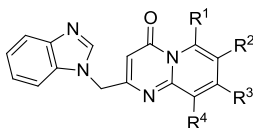
**Scheme 1:** Synthesis of pyridopyrimidinones analogs.

In order to further improve the PKM2 activation potency, the bound conformation of **4** was compared with other published conformations.<sup>13,9</sup> The benzimidazole ring of **4** appears to make favorable interactions with the neighboring residues of PKM2, therefore, we decided to keep this portion of the ligand constant in our optimization (figure 4). Opportunities to optimize hydrophobic interactions to the enzyme around the pyridopyrimidinone ring were identified and modeled. On the basis of docking scores, various analogs (compounds **8-13**, **Table 1**) were identified and synthesized following the route shown in **scheme 1**. In general, small substituents such as methyl, chloro or methoxy groups improved potency. small alkyl substitutions at C6 (R<sup>1</sup>) or C9 (R<sup>4</sup>) of the pyridopyrimidinone ring were especially effective.



**Figure 4.** Interactions of benzimidazole ring. Crystal structure of compound **4** (magenta) showing the  $\pi$ - $\pi$  interaction between Phenylalanines 26A (pink) and 26B (cyano), imidazole NH interaction to Lys B-311 and carbonyl interaction to Tyr390 via a water network. Only one binding mode shown.

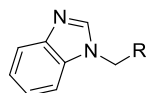
Due to the presence of  $\pi$ - $\pi$  interactions between the activators and phenylalanines 26A and 26B (**Figure 4**), we attempted to improve binding efficiency by altering the electron density of the pyridopyrimidinone portion of the activator core. Analogs with higher electron density (**12**, methoxy analog) or lower electron density (compounds **14-19**, thiazolo or thiodiazolo analogs, **Table 2**) were synthesized. The thiazolopyrimidinone ring appeared to have an electron density slightly more favorable for the  $\pi$ - $\pi$  interaction with the phenyl groups (e.g. compound **18**,  $AC_{50} = 266$  nM, compared to compound **4**,  $AC_{50} = 340$  nM). Consistent with earlier observations, small substitutions off the thiazolo portion of the thiazolo pyrimidinone ring seem to increase potency (e.g. **14**,  $AC_{50} = 86$  nM) whereas larger substitutions decrease potency (e.g. **15**,  $AC_{50} = 1.03$   $\mu$ M). Modeling compounds **12**, **15** and **19** into compound **4** crystal structure reveals a potential clash with residue GLN393 thus explaining their lost of potency.

**Tables 1. SAR and selected Pyridopyrimidinone analogs**

Compd	R <sup>1</sup>	R <sup>2</sup>	R <sup>3</sup>	R <sup>4</sup>	PKM2 AC <sub>50</sub> (uM) <sup>a</sup>	PKM2 Asymp max (%) <sup>b</sup>	HLM <sup>c</sup> (uL/min/mg)	RRCK (cm/sec) <sup>d</sup>	Solubility (uM) <sup>e</sup>	ClogP <sup>f</sup>	LipE
8	Me	H	H	H	0.159	198	<8	20.5	178	2.08	4.7
9	H	H	Me	H	0.216	161	13.3	21.3	586	2.08	4.6
10	H	Cl	H	H	0.219	156	<8	22.2	558	2.30	4.4
11	Me	H	H	Et	0.120	135	184	16.2	ND	3.10	3.8
12	H	OMe	H	H	0.470	123	<8	25.8	580	1.79	4.5
13	H	H	H	Me	0.145	172	17.8	24.2	529	2.08	4.8

<sup>a</sup> AC<sub>50</sub> values were determined in the lactate dehydrogenase (LDH) enzyme assay (ref.8). <sup>b</sup> PKM2 asymptote max represents the % activation at infinite compound concentration. <sup>c</sup> HLM corresponds to the intrinsic metabolic clearance (Clint) in microsomes (ref.7). <sup>d</sup> RRCK represents the passive permeability from A to B direction of a transwell assay. <sup>e</sup> kinetic solubility @ pH = 7.4. <sup>f</sup> ClogP calculated with ChemBioDraw by Cambridge Soft.

**Table 2. SAR of Thiazolo and Thiodiazolo Pyridopyrimidinone analogs**

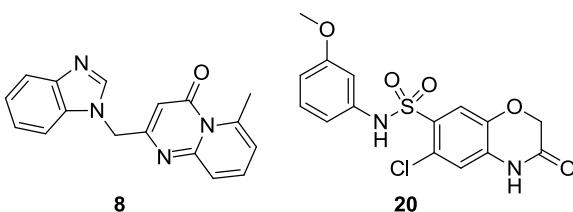


Compd	R	PKM2 AC <sub>50</sub> (uM) <sup>a</sup>	PKM2 Asymp max (%) <sup>b</sup>	HLM <sup>c</sup> (uL/min/mg)	RRCK (cm/sec) <sup>d</sup>	Solubility (uM) <sup>e</sup>	ClogP <sup>f</sup>	LipE
14		0.086	160	12.5	22.9	141	2.29	4.8
15		1.03	167	<8	11.5	ND	3.44	2.5
16		0.127	136	<8	23.4	117	1.84	5.1
17		0.466	189	<8	14.3	ND	1.84	4.5
18		0.266	162	<8	17.3	569	1.34	5.2
19		4.76	140	<8	17.6	ND	0.69	4.6

<sup>a</sup> AC<sub>50</sub> values were determined in the lactate dehydrogenase (LDH) enzyme assay (ref.8). <sup>b</sup> PKM2 asymptote max represents the % activation at infinite compound concentration. <sup>c</sup> HLM corresponds to the intrinsic metabolic clearance (Cl<sub>int</sub>) in microsomes (ref.7). <sup>d</sup> RRCK represents the passive permeability from A to B direction of a transwell assay. <sup>e</sup> kinetic solubility @ pH = 7.4. <sup>f</sup> ClogP calculated with ChemBioDraw by Cambridge Soft.

Through two rounds of optimization, both the potency and ligand efficiency were significantly improved from the original HTS hit (e.g. compound **1**, AC<sub>50</sub> = 3.47 uM, LE<sup>16</sup>=0.26, LipE=1.54 vs compound **8** AC<sub>50</sub> 0.159 uM, LE = 0.43, LipE = 4.7). Since many of the pyridopyrimidinone analogs are ligand efficient PKM2 activators with low molecular weight and lipophilicity, they generally demonstrated good ADME property profiles and favorable metabolic stability,<sup>17</sup> high permeability, and excellent aqueous solubility. Although the catalytic site of PKM2 is distinct from that of typical protein kinases,<sup>18</sup> we evaluated off-target liabilities by testing compound **8** across a selected panel of 35 kinases<sup>19</sup> at Life technologies, against a broad panel of pharmacological assays at CEREP,<sup>20</sup> as well as in the Ames

mutagenicity<sup>21</sup> assay. No positive findings were observed in any of these assays, suggesting compound **8** has no immediate evident liabilities.



	<b>8</b>	<b>20</b>
<b>HLMG (uL/min/mg):</b>	<8.0	22.4
<b>RRCK (x10<sup>-6</sup> cm/sec):</b>	20.5	8.80
<b>Sol@pH 6.5 (uM):</b>	178	8.6
<b>AC<sub>50</sub> (uM)</b>	0.159uM	0.153uM
<b>Max. Act.</b>	192%	108%
<b>Cell PK EC<sub>50</sub> (Huh7):</b>	0.0701	0.0222
<b>Tetramer formation (Huh7):</b>	Yes	Yes
<b>OCAR Change (%control)(10 uM):</b>	101.4%	85.7%
<b>ECAR Change (% control)(10 uM):</b>	108.9%	91.4%
<b>Anti-proliferation IC<sub>50</sub> (HT29):</b>	2.83%inh@10uM	26.8%inh@10uM

**Figure 5.** Profile comparison of pyridopyrimidinones lead **8** and a sulfonamide analog (**20**) previously reported to be a PKM2 activator (ref. 6c).

Compound **20**, a lead compound from another known series,<sup>6c</sup> and compound **8** were used as small molecule tools to probe the biological effects of PKM2 activation. Both compounds activated PKM2 in Huh7 cells [**8**, Cell PK EC<sub>50</sub> (Huh7) = 70 nM; **20**, Cell PK EC<sub>50</sub> (Huh7) = 22 nM, Figure 5].<sup>22</sup> As shown in Figure 6a, both compounds induced formation of PKM2 tetramers (240 kd vs. 60 kd monomer) in Huh7 cells. However, neither compound promoted any significant change in oxygen consumption (OCAR change) or lactate production (ECAR change) in Snu-182 (Figure 6b).<sup>23</sup> Furthermore, neither compound effectively suppressed cancer cell growth in Snu182, Snu449, Huh1 or JHH-2 cell lines, even at 10uM.<sup>24</sup>

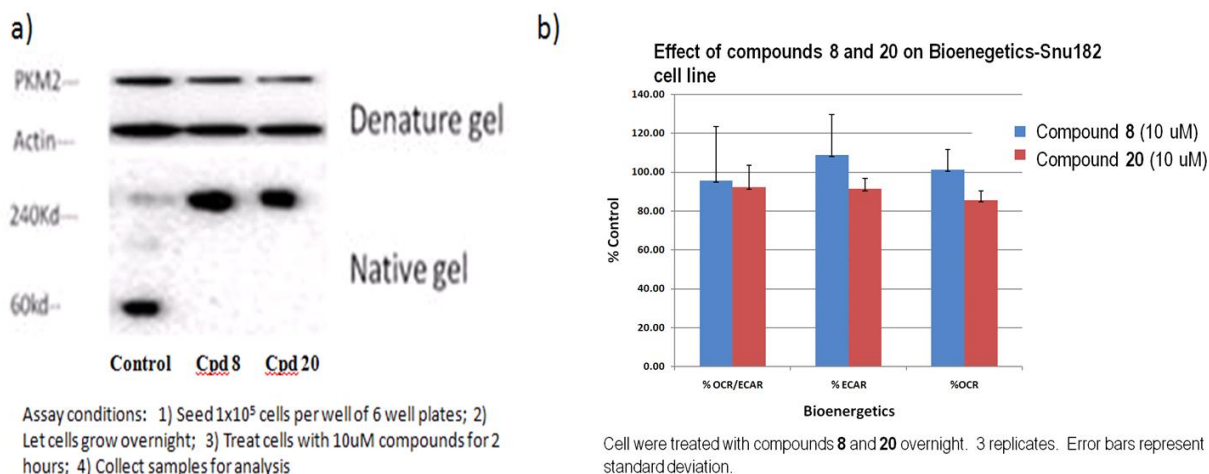


**Figure 6.** The Effect of PKM2 Activators 8 and 20 on PKM2. (a) Effect on tetramer (240kd band) formation in Huh7. (b) Effect in bioenergetics of Snu-182 cell line.

In summary, 2-((1*H*-benzo[*d*]imidazol-1-yl)methyl)-4*H*-pyrido[1,2-*a*]pyrimidin-4-ones are potent and selective PKM2 activators with a novel binding mode to the PKM2 protein. Both a representative compound from this series and an activator described in the literature<sup>6c</sup> were used as molecular tools to probe the biological effects of PKM2 activation on cancer cells. The two compounds activate PKM2 both enzymatically and cellularly, and induce tetramer formation, but they do not affect cancer cell glycolysis (OCAR/ECAR), and are not effective in suppressing cancer cell growth in vitro. While it is a formal possibility other chemotypes could induce a different tetrameric conformation, one that is functionally equivalent to the preferential expression of PKM1, our studies suggest that PKM2 activation alone is not sufficient to alter cancer cell metabolism and reverse the Warburg effect.

### Supplementary material

Supplementary material associated with this article can be found in the online version, at <http://dx.doi.org/XXXXXXXXX>. Material provided includes an illustration of the 4/PKM2 co-crystal structure showing both ligand binding conformations, as well as synthetic procedures and supporting spectral data for all numbered compounds and novel reactants.

### References and notes:

<sup>1</sup> Hanahan, D.; Weinberg, R. A. *Cell* **2011**, *144*, 646.

<sup>2</sup> Warburg, O. *Science* **1956**, *123*, 309.

<sup>3</sup> Christofk, H. R.; Vander Heiden, M. G.; Harris, M. H.; Ramanathan, A.; Gerszten, R. E.; Wei, R.; Fleming, M. D.; Schreiber, S. L.; Cantley, L. C. *Nature* **2008**, *452*, 230.

<sup>4</sup> (a) ref 3; (b) Mazurek, S.; Boschek, C. B.; Hugo, F.; Eigenbrodt, E. *Semin Cancer Biol.* **2005**, *15*, 300. (c) Dombrauckas, J. D.; Santarsiero, B. D.; Mesecar, A. D. *Biochemistry* **2005**, *44*, 9417. (d) Mazurek, S. *Int. J. Biochem. Cell Biol.* **2011**, *43*, 969.

<sup>5</sup> (a) Levine, A. J.; Puzio-Kuter, A. M. *Science* **2010**, *330*, 1340. (b) Vander Heiden, M. G.; Cantley, L. C.; Thompson, C. B. *Science* **2009**, *324*, 1029. (c) Luo, W.; Hu, H.; Chang, R.; Zhong, J.; Knabel, M.; O'Meally, R.; Cole, R. N.; Pandey, A.; Semenza, G. L. *Cell* **2011**, *145*, 732. (d) Gao, X.; Wang, H.; Yang, J. J.; Liu, X.; Liu, Z. R. *Mol. Cell* **2012**, *45*, 598. (e) Anastasiou, D.; Yu, Y.; Israelsen, W. J.; Jiang, J.-K.; Boxer, M. B.; Hong, B. S.; Tempel, W.; Dimov, S.; Shen, M.; Jha, A.; Yang, H.; Mattaini, K. R.; Metallo, C. M.; Fiske, B. P.; Courtney, K. D.; Malstrom, S.; Khan, T. M.; Kung, C.; Skoumbourdis, A. P.; Veith, H.; Southall, N.; Walsh, M. J.; Brimacombe, K. R.; Leister, W.; Lunt, S. Y.; Johnson, Z. R.; Yen, K. E.; Kunii, K.; Davidson, S. M.; Christofk, H. R.; Austin, C. P.; Inglese, J.; Harris, M. H.; Asara, J. M.; Stephanopoulos, G.; Salituro, F. G.; Jin, S.; Dang, L.; Auld, D. S.; Park, H.-W.; Cantley, L. C.; Thomas, C. J.; Vander Heiden, M. G. *Nature Chem. Biol.* **2012**, *8*, 839. (f) Cortés-Cros, M.; Hemmerlin, C.; Ferretti, S.; Zhang, J.; Gounarides, J. S.; Yin, H.; Muller, A.; Haberkorn, A.; Chene, P.; Sellers, W. R.; Hofmann, F. *Proc. Natl. Acad. Sci. U.S.A.* **2013**, *110*, 489. (g) Baas, T. *SciBX*, **2013**, *6*(2); doi:10.1038/scibx.2013.28. Published online Jan. 17, 2013.

<sup>6</sup> (a) Boxer, M. B.; Jiang, J. K.; Vander Heiden, M. G.; Shen, M.; Skoumbourdis, A. P.; Southall, N.; Veith, H.; Leister, W.; Austin, C. P.; Park, H. W.; Inglese, J.; Cantley, L. C.; Auld, D. S.; Thomas, C. J. *J. Med. Chem.* **2010**, *53*, 1048. (b) Jiang, J.-K.; Boxer, M. B.; Vander Heiden, M. G.; Shen, M.; Skoumbourdis, A. P.; Southall, N.; Veith, H.; Leister, W.; Austin, C. P.; Park, H. W.; Inglese, J.; Cantley, L. C.; Auld, D. S.; Thomas, C. J. *Bioorg. Med. Chem. Lett.* **2010**, *20*, 3387. (c) Walsh, M. J.; Brimacombe, K. R.; Veith, H.; Bougie, J. M.; Daniel, T.; Leister, W.; Cantley, L. C.; Israelsen, W. J.; Vander Heiden, M. G.; Shen, M.; Auld, D. S.; Thomas, C. J.; Boxer, M. B. *Bioorg. Med. Chem. Lett.* **2011**, *21*, 6322.

<sup>7</sup> HLM corresponds to the intrinsic metabolic clearance (Cl<sub>int</sub>) in microsomes, in uL/min/mg of microsomal protein. Data interpretation as following: Cl<sub>int</sub> <15 uL/min/mg (low clearance); Cl<sub>int</sub> 15-40 uL/min/mg (moderate clearance); Cl<sub>int</sub> >40 (high clearance).

<sup>8</sup> The Pyruvate Kinase-catalyzed production of ATP that accompanies phosphoryl transfer from PEP substrate to ADP is coupled to the oxidation of β-NADH through the action of lactate dehydrogenase (LDH). NADH

conversion to NAD<sup>+</sup> is monitored by the decrease in absorbance at 340 nm ( $\Delta\epsilon = 6.22 \text{ mM}^{-1}\text{cm}^{-1}$ ) using a Molecular Devices Spectramax Plus plate reader. Typical reaction solutions contain 2nM PK enzyme (human PKM2 (cleaved N-term his, 1-531), (~2X Km concentration), 2 mM PEP (~Km of PKM2 minus FBP), 0.35 mM NADH, and 4 units/mL LDH in 50 mM Tris buffer, pH 7.5 containing 100mM KCl<sub>2</sub> and 5 mM MgCl<sub>2</sub>. Compound or DMSO is added to appropriate wells and allowed to incubate for 10 minutes at 32 °C. The reaction is initiated with 0.5mM ADP. Percent inhibition/activation is determined in duplicate at an appropriate inhibitor concentration. For IC<sub>50</sub>/AC<sub>50</sub> determinations, compounds are typically run at 10 concentration points (including no inhibitor control, no enzyme control, and activator control) using a 1:3 serial dilution starting from 100 μM (for original HTS “hits” and exploratory compounds) or 1:2 serial dilution from 10 μM (for more potent compounds from targeted libraries).

<sup>9</sup> Docking methods and examples see following references. (a) Guo, C.; Hou, X.; Dong, L.; Dagostino, E.; Greasley, S.; Ferre, R.; Marakovits, J.; Johnson, M.C.; Matthews, D.; Mroczkowski, B.; Parge, H.; VanArsdale, T.; Popoff, I.; Piraino, J.; Margosiak, S.; Thomson, J.; Los, G.; Murray, B.W. *Bioorg. Med. Chem. Lett.* **2009**, *19*, 5613. (b) Dong, L.; Marakovits, J.; Hou, X.; Guo, C.; Greasley, S.; Dagostino, E.; Ferre, R.; Johnson, M.C.; Kraynov, E.; Thomson, J.; Pathak, V.; Murray, B.W. *Bioorg. Med. Chem. Lett.* **2010**, *20*, 2210.

<sup>10</sup> Published PKM2 co-crystal structures are found in the Protein Data Bank. The protein shown corresponds to PDB IDs = 3GQY.

<sup>11</sup> a) Ryckmans, T.; Edwards, M.E.; Horne, V.A.; Correia, A.M.; Owen, D.R.; Thompson, L.R., Tran, I.; Tutt, M.F.; Young, T. *Bioorg. Med. Chem. Lett.* **2009**, *19*, 4406. b) Guo, C.; Linton, A.; Kephart, S.; Ornelas, M.; Pairish, M.; Gonzalez, J.; Greasley, S.; Nagata, A.; Burke, B.J.; Edwards, M.; Hosea, N.; Kang, P.; Hu, W.; Engebretsen, J.; Briere, D.; Shi, M.; Gukasyan, H.; Richardson, P.; Dack, K.; Underwood, T.; Johnson, P.; Morell, A.; Felstead, R.; Kuruma, H.; Matsimoto, H.; Zoubeidi, A.; Gleave, M.; Los, G.; Fanjul, A.N. *J. Med. Chem.* **2011**, *54*, 7693. c) Guo, C.; Kephart, S.; Ornelas, M.; Gonzales, J.; Linton, A.; Pairish, M.; Nagata, A.; Greasley, S.; Elleraas, J.; Hosea, N.; Engebretsen, J.; Fanjul, A.N. *Bioorg. Med. Chem. Lett.* **2012**, *22*, 1230. d) Guo, C.; Pairish, M.; Linton, A.; Kephart, S.; Ornelas, M.; Nagata, A.; Burke, B.; Dong, L.; Engbretsen, J.; Fanjul, A.N. *Bioorg. Med. Chem. Lett.* **2012**, *22*, 2572. e) Guo, C.; McAlpine, I.; Zhang, J.; Knighton, D.; Kephart, S.; Johnson, M.C.; Li, H.; Bouzida, D.; Yang, A.; Dong, L.; Marakovits, J.; Tikhe, J., Richardson, P., Guo, L.; Kania, R.; Edwards, M.; Kraynov, E.; Christensen, J.; Piraino, J.; Lee, J.; Dagostino, E.; Del-Carmen, C., Deng, Y.; Smeal, T.; Murray, B.W. *J. Med. Chem.* **2012**, *55*, 4728.

<sup>12</sup> The PDB code of the structure is 4JPG. The ligand was solved with a 2.33 Å resolution. The ligand is bound in the A/B dimer activator site, bound in 2 conformations with equal occupancy. The ligand was also found in the C/D dimer. Compared to apo and other activator-bound structures, there were no significant changes in the conformation of residues in the activator site.

<sup>13</sup> Published PKM2 co-crystal structures are found in the Protein Data Bank. Structures shown corresponds to PDB IDs = 3GR4, 3H6O and 3GQY.

<sup>14</sup> For density map of the two ligand binding conformations see Figure S1 in the Supplementary Material.

<sup>15</sup> For experimental procedures, including synthesis of non-commercially available reactants, see Supplementary Material.

<sup>16</sup> Kuntz, I. D.; Chen, K.; Sharp, K. A.; Kollman, P. A. *Proc. Natl. Acad. Sci. U.S.A.* **1999**, *96*, 9997.

<sup>17</sup> The 2-((1*H*-benzo[d]imidazol-1-yl)methyl)-4*H*-pyrido[1,2-*a*]pyrimidin-4-ones core was found to be a substrate of aldehyde oxydase (AO), which may present challenges in clinical development. The AO assay was described in following reference. Linton, A.; Kang, P.; Ornelas, M.; Kephart, S.; Hu, Q.; Pairish, M.; Jiang, Y.; Guo, C. *J. Med. Chem.* **2011**, *54*, 7705.

<sup>18</sup> PKM2 is one of the Pyruvate Kinases. Pyruvate Kinases do not phosphorylate other proteins, rather a pyruvate kinase catalyzes the transfer of a phosphate group from phosphoenolpyruvate (PEP) to ADP, generating ATP and pyruvate. Its substrate is PEP, not ATP (protein kinase substrate). Therefore, the catalytic site of Pyruvate Kinases (including PKM2) is distinct from that of protein kinases. For example, the PKM2 catalytic site does not contain a hinge-binding motif, a highly conserved area for classic protein kinases.

<sup>19</sup> Selected kinase panel: ABL1, AKT1 (PKB alpha), AURKA (Aurora A), BTK, CAMK2A (CaMKII alpha), CDK2/cyclin A, CHEK1 (CHK1), CHEK2 (CHK2), CSNK1A1 (CK1 alpha 1), CSNK2A2 (CK2 alpha 2), EGFR (ErbB1), EPHA2, FGFR1, GSK3B (GSK3 beta), INSR, JAK3, KDR (VEGFR2), LCK, MAP4K4 (HGK), MAPK1 (ERK2), p38, MAPKAPK2, MARK1 (MARK), MET (cMet), MST4 ,MYLK2 (skMLCK), NEK2, NTRK1 (TRKA), PAK4, PDK1 Direct, PIM2, PRKACA, (PKA), PRKCB2 (PKC beta II), ROCK1, SGK (SGK1), SRC, STK3 (MST2), TAOK2 (TAO1), TEK (Tie2), ZAP70, mTOR, PIK3C2A (PI3K-C2 alpha).

<sup>20</sup> CEREP panel: Alpha 1 (non-selective) (antagonist radioligand), Beta 2 (h) (agonist radioligand), D1 (h) (antagonist radioligand), Dopamine transporter (h) (antagonist radioligand), Muscarinic M1 (h) (antagonist radioligand), mu opiod (MOP) (h) (agonist radioligand), Ca<sup>2+</sup> channel (L, diltiazem site) (benzothiazepines) (antagonist radioligand), Na<sup>+</sup> channel (site 2) (antagonist radioligand), norepinephrine transporter (h) (antagonist radioligand), 5-HT transporter (h) (antagonist radioligand), Histamine H1 (h) (antagonist radioligand), 5-HT2B (h) (agonist radioligand), PDE3B (h), Cannabiniod CB1, GABA-BZD (central) rat cerebral cortex.

<sup>21</sup> Ames assay conditions were reported previously. Palmer, C.; Pairish, M.; Kephart, S.; Bouzida, D.; Cui, J.; Deal, J.; Dong, L.; Gu, D.; Linton, A.; McAlpine, I.; Yamazaki, S.; Smith, E.; John-Baptiste, A.; Bagrodia, S.; Kania, R.; Guo, C. *Bioorg. Med. Chem. Lett.* **2012**, *22*, 7605.

<sup>22</sup> In this assay, cells from the human HCC cell line, Huh7 were treated with the test compounds, and then lysed cells were added to PEP and ADP to generate pyruvate and ATP. The generated pyruvate was oxidized by pyruvate oxidase to produce fluorescence. Since the increase in fluorescence intensity is proportional to the increase in pyruvate concentration, the pyruvate kinase activity from cells was accurately measured.

<sup>23</sup> Compound Effect on Bioenergetic Profile: To determine compounds' effect on bioenergetic profile, the oxygen consumption rate (OCR) and extracellular acidification rate (ECAR) of Snu182 cells treated with compounds was measured. Snu182 cells were seeded at density of 12k/well with RPMI growth media (Life Technology, #21870) supplemented with 10% FBS and 2 mM Glutamine in 96-well polyethylene terephthalat (PET) microplates (Seahorse Bioscience, #101107-001). After overnight culture, 10  $\mu$ M compounds were added to the media. After 18 hours culture at 37°C and 5% CO<sub>2</sub>, the media was changed to XF DMEM media (Seahorse, #100965-000) that was supplemented 5 mM Glucose and 10  $\mu$ M compounds, OCR and ECAR readouts were assayed on the Seahorse XF96 Analyzer.

<sup>24</sup> Anti-proliferation assay. Cells were seeded in 96-well plates with Optimem-GlutaMax media (Invitrogen). After overnight culture, 10  $\mu$ M compound **8** and **20** were added to the cells. Cell viability was measured by Cyto Tox-Glo kit (Promega) after 5-day compound treatment.